Search for dark matter in association with a Higgs boson decaying to two photons at sqrt(s) = 13 TeV with the ATLAS detector

(My) personal motivation to pick up this topic

- When investigage dark photon (A'), we can find also the contents about dark Z (Z') since both can be mixing basically

  -- What is Z' ?

  -- Which experiments or what is the results from Z' search ?

  -- What is base of those model ?

  -- Is there any impact for dark matter model for J/psi->invisible ?

  -- ....

Model Assumption

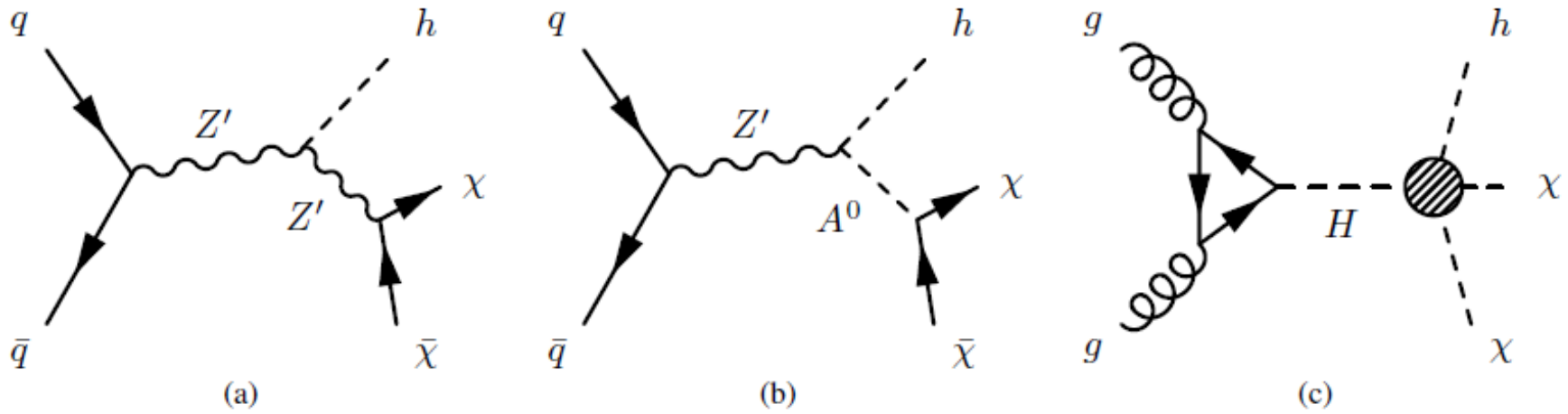

Figure 1: The Feynman diagrams for the production of DM (χ) in association with a SM Higgs boson (h) arising from three theoretical models considered in this paper: (a) Z'_B model, (b) Z'-2HDM model, (c) heavy-scalar model.

2HDM (two-Higgs doublet model) : additional Higgs particles.

--→ the point maybe , , , modified Lagrangian can have $Z'A^0*h$ term, though h is normal Higgs

Reference slide :

Benchmark Models

ATLAS-CMS Dark Matter (DM) Forum *arXiv:1507.00966*

➔ define benchmark models for kinematically distinct signals for Run-2 searches:

"Simplified" models:

- DM particle is a Dirac fermion, χ
- Mediator (med) exchanged in the s-channel
- 5 parameters: M_{med}, m_{χ}, g_q, g_{χ}, Γ_{med}
- Physics objects (X) produced in ISR
- Specific model for X=Higgs (h):
  - Mediator radiates h and decays to $\chi\chi$

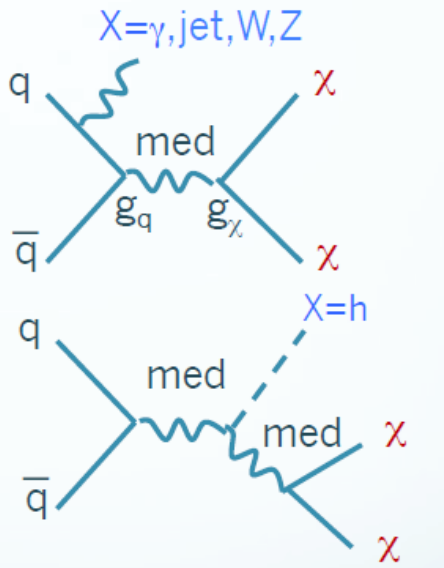

EFT models:

- Valid if the M_{med} >> momentum transfer at LHC
- Specific EW EFT model:
  - direct coupling betweeen DM and EW bosons
  - motivate searches with EW final states

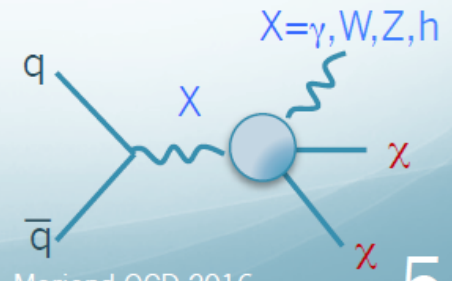

Analysis (Event selection)

Concept : identification of Higgs via di-photon, along with large E^{miss}_T .

They classify the set into 5 categories , , ,

The selected events are thus divided into five categories based on:

- the E_T^{miss} significance, $S_{E_T^{miss}} = E_T^{miss} / \sqrt{\sum E_T}$, where the total transverse energy $\sum E_T$ is calculated from the scalar sum of the transverse momenta of the calibrated photons, electrons, muons and jets used in the E_T^{miss} calculation described in Section 4, as well as the tracks not associated with these but the PV;
- the diphoton transverse momentum, $p_T^{\gamma\gamma}$;
- p_T^{hard};
- the number of leptons in the event;
- the distance between the diphoton vertex and the highest Σp_T^2 vertex in the z direction: $|z_{PV}^{highest} - z_{PV}^{\gamma\gamma}|$.

Table 1: Optimized criteria used in the categorization. The categories are defined sequentially in the rows and each category excludes events in the previous row.

Category	Requirements
Mono-Higgs	$S_{E_T^{miss}} > 7\ \sqrt{\text{GeV}}$, $p_T^{\gamma\gamma} > 90$ GeV, lepton veto
High-E_T^{miss}	$S_{E_T^{miss}} > 5.5\ \sqrt{\text{GeV}}$, $\lvert z_{PV}^{highest} - z_{PV}^{\gamma\gamma}\rvert < 0.1$ mm
Intermediate-E_T^{miss}	$S_{E_T^{miss}} > 4\ \sqrt{\text{GeV}}$, $p_T^{hard} > 40$ GeV, $\lvert z_{PV}^{highest} - z_{PV}^{\gamma\gamma}\rvert < 0.1$ mm
Different-Vertex	$S_{E_T^{miss}} > 4\ \sqrt{\text{GeV}}$, $p_T^{hard} > 40$ GeV, $\lvert z_{PV}^{highest} - z_{PV}^{\gamma\gamma}\rvert > 0.1$ mm
Rest	$p_T^{\gamma\gamma} > 15$ GeV

(Supporting) Distribution of various parameters

Z’-2HDM model has relatively large E_{miss} … ?

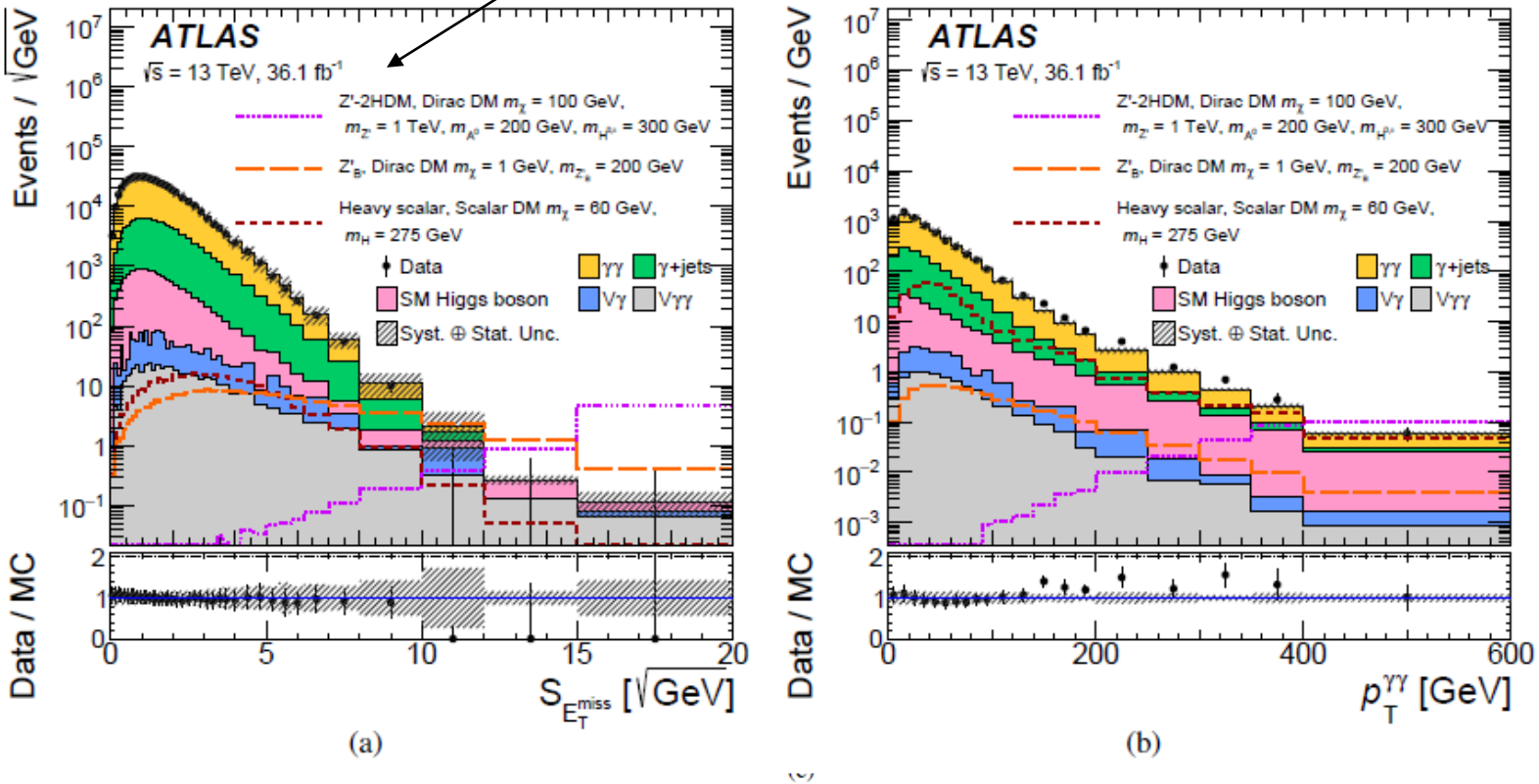

Figure 2: The distribution of (a) $S_{E_T^{miss}}$, (b) $p_T^{\gamma\gamma}$ and (c) p_T^{hard} after the selection of diphoton candidates in 120 GeV < $m_{\gamma\gamma}$ < 130 GeV. Expected distributions are shown for a Z'_B signal with $m_{Z'_B}$ = 200 GeV and Dirac fermion DM m_χ = 1 GeV; a Z'-2HDM signal with $m_{Z'}$ = 1000 GeV, m_{A^0} = 200 GeV and Dirac fermion DM m_χ = 100 GeV; and a heavy-scalar model with m_H = 275 GeV and scalar DM m_χ = 60 GeV. These overlaid signal points are representative of the model kinematics. Only the quadratic sum of the MC statistical and experimental systematic uncertainties in the total background is shown as the hatched bands, while the theoretical uncertainties in the background normalization are not included. Overflow events are included in the rightmost bin. The asymmetric error bars on data points come from Poissonian confidence intervals at 68% confidence level.

Result . Example distribution of di-photon invariant mass for Z'_B model

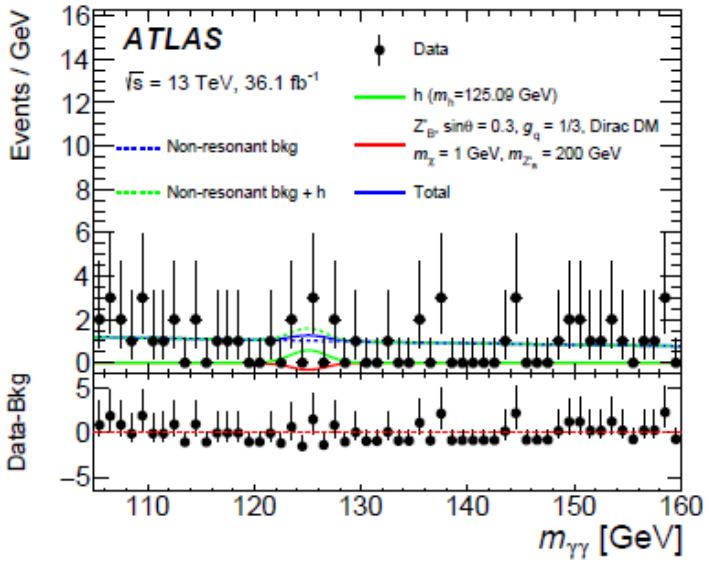

Figure 3: Diphoton invariant mass distribution for data and the corresponding fitted signal and background in the Mono-Higgs category for the Z'_B benchmark model fit using $g_q = 1/3$, $g_\chi = 1$, $\sin\theta = 0.3$ and Dirac fermion DM $m_\chi = 1$ GeV as an illustration. A negative best-fit DM signal is found. The data is shown as dots with asymmetric error bars that represent central Poissonian confidence intervals at 68% CL. The fitted signal (solid red line), SM Higgs boson (solid green line), non-resonant background (dashed blue line) and the non-resonant background plus the SM Higgs boson (dashed green line) are shown as well as the total of all those contributions (solid blue line).

C.L. on the cross-section

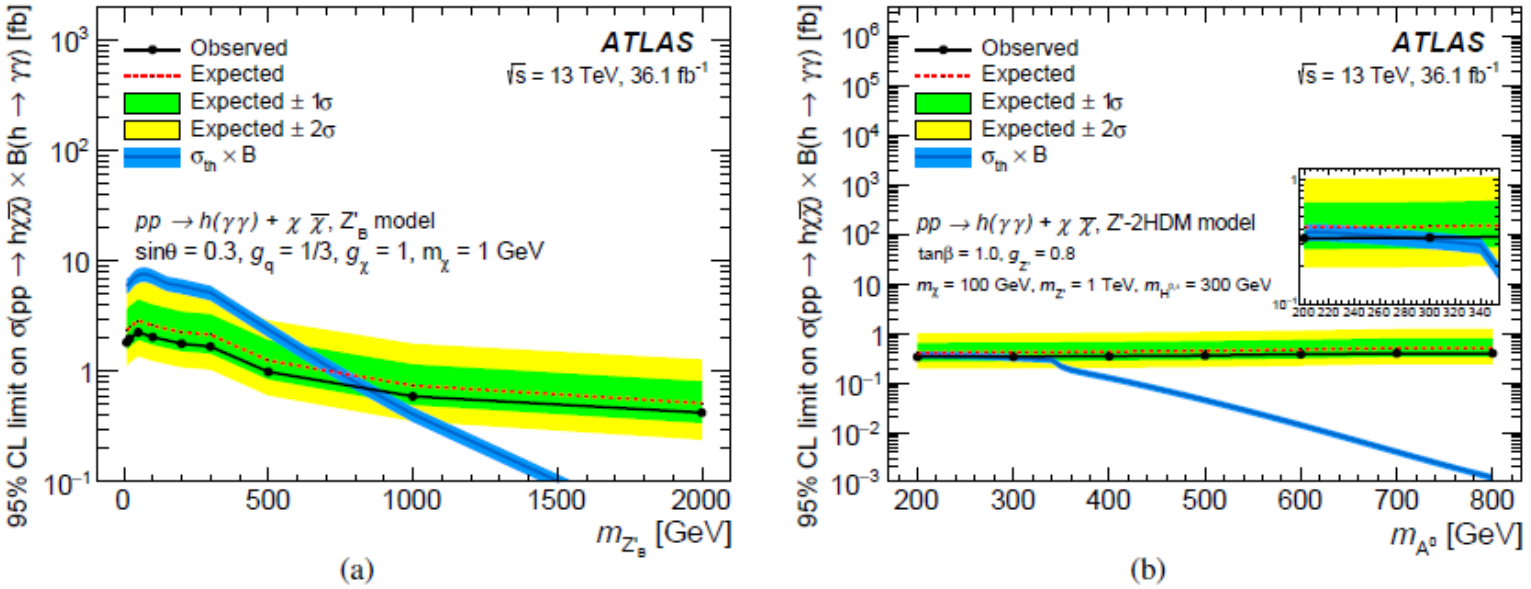

Figure 4: Expected (dashed lines) and observed (solid lines) 95% CL upper limits on $\sigma(pp \to h\chi\bar{\chi}) \times \mathcal{B}(h \to \gamma\gamma)$ for (a) the Z'_B model for $g_q = 1/3$, $g_\chi = 1$, $\sin\theta = 0.3$ and Dirac fermion DM $m_\chi = 1$ GeV and (b) the Z'-2HDM model for $\tan\beta = 1$, $g_{Z'} = 0.8$, $m_{Z'}$=1000 GeV and Dirac fermion DM $m_\chi = 100$ GeV, as a function of $m_{Z'_B}$ and m_{A^0}, respectively. The masses of the neutral CP-even scalar (H^0) and the charged scalars ($H^\pm$) from Z'-2HDM model are set to 300 GeV. The theoretical predictions of $\sigma(pp \to h\chi\bar{\chi}) \times \mathcal{B}(h \to \gamma\gamma)$ for these two models (dark-blue lines with blue bands representing their associated theoretical systematic uncertainties) are also shown. The inset shows a zoomed-in view of the same figure in narrower ranges of both the x and y axes.

C.L. on the cross-section
(heavy scaler model)

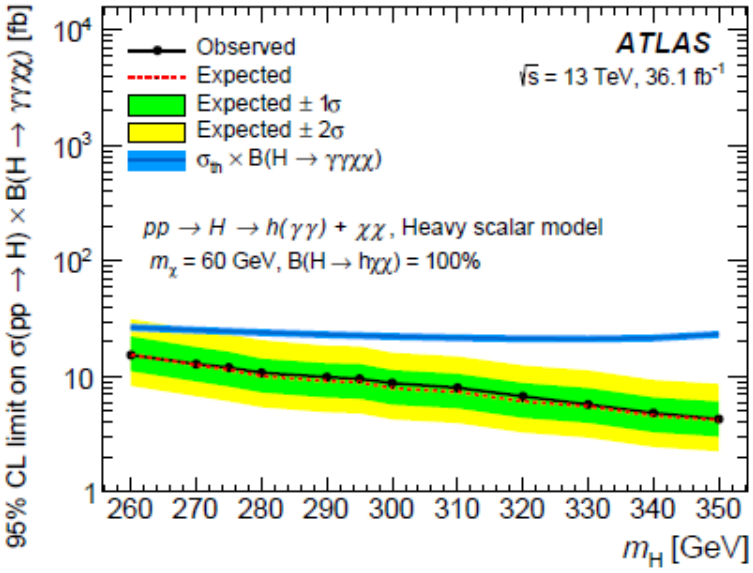

Figure 8: Observed and expected 95% CL upper limits on the $\sigma(pp \to H) \times \mathcal{B}(H \to \gamma\gamma\chi\chi)$ with a scalar DM candidate mass of 60 GeV as a function of the heavy-scalar-boson mass in the range 260 GeV $< m_H <$ 350 GeV. A 100% branching fraction is assumed for $H \to h\chi\chi$. The theoretical prediction for the model (dark-blue lines with blue bands representing their associated theoretical systematic uncertainties) is also shown. The theoretical cross section is assumed to be equal to that of a SM Higgs boson with the same mass produced in gluon–gluon fusion.

C.L. on 2-dimentional map

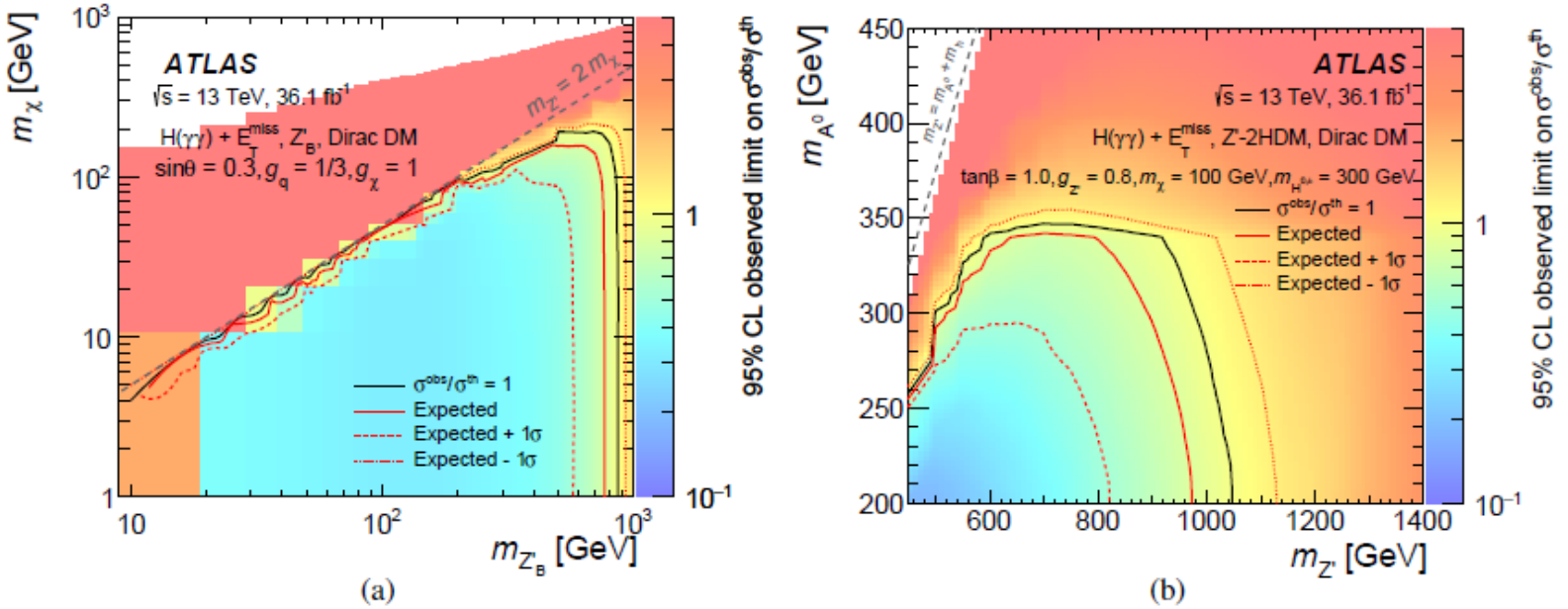

Figure 5: The ratios of the observed and expected 95% CL upper limits on the signal cross section to the predicted signal cross sections for (a) the Z'_B model in the (m_χ, $m_{Z'_B}$) plane and (b) the Z'-2HDM model in the (m_{A^0}, $m_{Z'}$) plane. For the Z'_B model, the mixing angle $\sin\theta = 0.3$, and the coupling values $g_q = 1/3$ and $g_\chi = 1$ are used. In the scenario of Z'-2HDM model, the ratio of the two-Higgs-doublet vacuum expectation values $\tan\beta = 1.0$, Dirac fermion DM mass $m_\chi = 100$ GeV, and the coupling value $g_{Z'} = 0.8$ are used. The masses of the neutral CP-even scalar (H^0) and the charged scalars ($H^\pm$) from Z'-2HDM model are set to 300 GeV. The plus and minus one standard deviation expected exclusion curves are also shown as red dashed and dotted lines. The regions below the lines (i.e. with $\sigma^{\text{obs}}/\sigma^{\text{th}} < 1$) are excluded. In both figures, the gray dashed line corresponds to the boundary of the region above which the Z' boson is produced off-shell.

Comparison with the other experiments

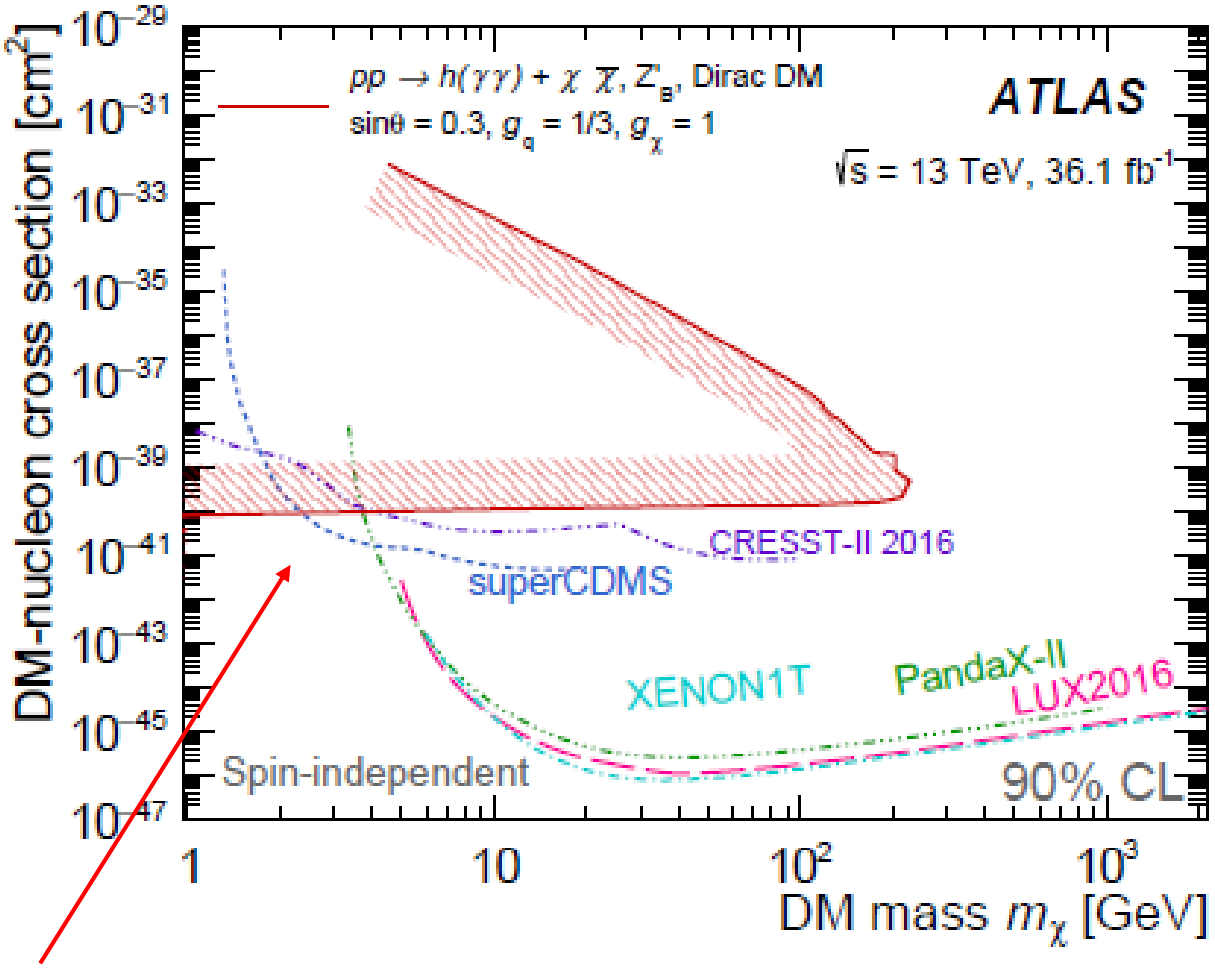

・I don't fully understand why the exclusion area becomes "circle"

・At any rate, it shows that at low mass, it has potential to set better limit than those experiments.

Summary

A search for dark matter in association with a Higgs boson decaying to two photons is presented. This study is based on data collected with the ATLAS detector, corresponding to an integrated luminosity of 36.1 fb^{-1} of proton–proton collisions at the LHC at a center-of-mass energy of 13 TeV in 2015 and 2016. No significant excess over the expected background is observed. For the Mono-Higgs category, a visible cross section larger than 0.19 fb is excluded at 95% CL for BSM physics processes producing missing transverse momentum and a SM Higgs boson decaying into two photons. Upper limits at 95% CL are also set on the production cross section times branching fraction of the Higgs boson decaying into two photons in association with missing transverse momentum in three different benchmark models: a Z'_B model, a Z'-2HDM model and a heavy scalar boson (H) model. Limits at 95% CL are also set on the observed signal strength in a two-dimensional m_χ–$m_{Z'_B}$ plane for the Z'_B model, and the m_{A^0}–$m_{Z'}$ plane for the Z'-2HDM model. Additionally, the results for the Z'_B model are interpreted in terms of 90% CL limits on the dark-matter–nucleon scattering cross section, as a function of the dark matter particle mass, for a spin-independent scenario. For a dark-matter mass lower than 2.5 GeV, the constraint with couplings $g_q = 1/3$ and $g_\chi = 1$ placed on the DM–nucleon cross section is more stringent than limits from direct detection experiments. In the model involving the production of a heavy scalar boson, 95% CL upper limits are set on the production cross section times the branching fraction of $H \to h\chi\chi \to \gamma\gamma\chi\chi$ for a dark-matter particle with mass of 60 GeV, where a 100% branching fraction is assumed for $H \to h\chi\chi$. The heavy-scalar model assuming H production through gluon–gluon fusion with a cross section identical to that of a SM Higgs boson of the same mass, is excluded for all the benchmark points investigated.